The Candidate Schizophrenia Risk Gene *DGCR2* Regulates Early Steps of Corticogenesis

Molinard-Chenu, Aude; Dayer, Alexandre

How to cite

MOLINARD-CHENU, Aude, DAYER, Alexandre. The Candidate Schizophrenia Risk Gene *DGCR2* Regulates Early Steps of Corticogenesis. In: Biological Psychiatry, 2018, vol. 83, n° 8, p. 692–706. doi: 10.1016/j.biopsych.2017.11.015

This publication URL: https://archive-ouverte.unige.ch/unige:124259
Publication DOI: 10.1016/j.biopsych.2017.11.015

Biological Psychiatry

Archival Report

The Candidate Schizophrenia Risk Gene *DGCR2* Regulates Early Steps of Corticogenesis

Aude Molinard-Chenu and Alexandre Dayer

ABSTRACT

BACKGROUND: Alterations in early steps of cortical circuit assembly are thought to play a critical role in vulnerability to schizophrenia (SZ), but the pathogenic impact of SZ-risk mutations on corticogenesis remains to be determined. DiGeorge syndrome critical region 2 (*DGCR2*) is located in the 22q11.2 locus, whose deletion is a major risk factor for SZ. Moreover, exome sequencing of individuals with idiopathic SZ identified a rare missense mutation in *DGCR2*, further suggesting that *DGCR2* is involved in SZ.

METHODS: Here we investigated the function of *Dgcr2* and the pathogenic impact of the SZ-risk *DGCR2* mutation in mouse corticogenesis using in utero electroporation targeted to projection neurons.

RESULTS: *Dgcr2* knockdown impaired radial locomotion and final translocation of projection neurons, leading to persistent laminar positioning alterations. The *DGCR2* missense SZ-risk mutation had a pathogenic impact on projection neuron laminar allocation by reducing protein expression. Mechanistically, we identified *Dgcr2* as a novel member of the Reelin complex, regulating the phosphorylation of Reelin-dependent substrates and the expression of Reelin-dependent transcriptional targets.

CONCLUSIONS: Overall, this study provides biological evidence that the SZ-risk gene *DGCR2* regulates critical steps of early corticogenesis possibly through a Reelin-dependent mechanism. Additionally, we found that the SZ-risk mutation in *DGCR2* has a pathogenic impact on cortical formation by reducing protein expression level, suggesting a functional role for DGCR2 haploinsufficiency in the 22q11.2 deletion syndrome.

Keywords: 22q11, Corticogenesis, DGCR2, Neuronal migration, Reelin, Schizophrenia

https://doi.org/10.1016/j.biopsych.2017.11.015

Alterations in the formation of cortical circuits are involved in the pathophysiology of developmental disorders, including schizophrenia (SZ) (1,2). Numerous genes are associated with SZ (3,4) and many of them regulate cellular events involved in cortical circuit assembly (5,6). However, the precise biological mechanisms through which SZ-risk genes alter early cortical circuit formation remain unclear (7). Here, we investigate the impact of a novel SZ-risk gene, DiGeorge syndrome critical region 2 (*Dgcr2*), on cortical projection neuron (PN) development. *Dgcr2* is expressed throughout brain development (8), encodes for an activity-dependent adhesion protein (9,10), and is associated with SZ (3,11). *DGCR2* is located in the 22q11.2 locus, in the minimal critical region for 22q11.2 microdeletion syndrome (22q11.2DS) (12). This microdeletion is one of the highest known risk factors for SZ (13), and it has been suggested that *DGCR2* haploinsufficiency may contribute to increased risk for SZ in 22q11.2DS (11). Additionally, exome sequencing of family trios identified a rare de novo *DGCR2* mutation (P429R) in a patient with idiopathic SZ (3). Here we used in utero electroporation in mice (14,15) to determine whether *Dgcr2* impacts early steps of PN development and assessed the pathogenic impact of the *DGCR2* SZ-risk mutation in this model system.

Early cellular events involved in the development of cortical PNs are increasingly well understood (16,17). After being generated asymmetrically from radial glia in the ventricular zone, upper-layer PNs undergo sequential migratory stages until they reach their final laminar position within the cerebral cortex. A key stage in neuronal migration is radial glia–guided locomotion during which PNs migrate from the intermediate zone toward upper cortical layers (18). The fine positioning of PNs relies on an ultimate migratory step defined as final translocation (19). The precisely orchestrated migration of PNs appears to be a vulnerable cellular process that is affected by different types of psychiatric-related genetic insults (20–22).

Multiple cell-extrinsic regulators of PN migration have been identified (23,24). Among these factors, Reelin is an important signaling protein secreted by Cajal-Retzius cells (25). It controls the inside-out lamination of cortical PNs (26), and alterations in downstream signaling components of the Reelin pathway, such as *DAB1*, disturb radial glia-guided locomotion (27) and final translocation (20,28,29). Interestingly, the Reelin signaling cascade is associated with several SZ-related processes including *N*-methyl-D-aspartate receptor hypofunction (30–32) and SZ-like cognitive impairments (33–35).

SEE VIDEO CONTENT ONLINE

ISSN: 0006-3223

In this study, we find that short hairpin RNA (shRNA)–mediated knockdown (KD) of *Dgcr2* as well as an SZ-risk mutation in *DGCR2* affects the migration of PNs. Moreover, we identify DGCR2 as a novel member of the Reelin complex and show that the phosphorylation of Reelin-dependent signaling targets is reduced following *Dgcr2* KD. Finally, using RNA sequencing of *Dgcr2*-KD PNs, we identify *Dgcr2*-dependent target genes, which are significantly enriched in Reelin-dependent genes. Overall, this study provides evidence that the SZ-risk gene *Dgcr2* regulates PN migration and positioning possibly through Reelin-dependent mechanisms.

METHODS AND MATERIALS

Plasmids, antibodies, and primers are discussed in Supplemental Methods.

In Utero Electroporation

Animal experiments were conducted according to the Swiss and international guidelines and were approved by the local animal care committee. Embryos from time pregnant E14.5 CD1 mice or C57BL/6 (RNA sequencing experiment and Figure 1A) were electroporated in the lateral ventricular zone of the dorsal pallium as described previously (36). Sequential electroporations were performed at 24-hour intervals at E14.5 and E15.5.

Tissue Processing, Immunohistochemistry, and Proximity Ligation Assay

Dissected brains were fixed, stored in a cryoprotective solution if required, and processed for immunohistochemistry as described previously (22,36) and for proximity ligation assay (PLA) as described in Trifilieff *et al.* (37) with Duolink reagents (Sigma-Aldrich, St. Louis, MO).

Cell Culture and Transfection

Human embryonic kidney (HEK) 293T cells were cultured in Dulbecco's modified Eagle medium (Life Technologies, Carlsbad, CA) supplemented with 10% fetal bovine serum (Biochrom, Berlin, Germany), 10 U/mL penicillin/streptomycin mixture (Life Technologies) at 37°C under 5% CO_2. Cells were transfected using lipofectamin-2000 (Thermo Fisher Scientific, Waltham, MA). Primary neuronal cultures were prepared as previously described (36).

Western Blot and Immunoprecipitation

Cells were scraped and lysed in cell lysis buffer B. The lysate was clarified by centrifugation and 50 μg of proteins were processed as in Riccio *et al.* (36). For the coimmunoprecipitation experiment, Reelin-enriched medium was produced and collected as described in D'Arcangelo *et al.* (38) and after 1-hour incubation with Reelin-enriched or mock medium, transfected HEK 293T cells were resuspended in 0.4% paraformaldehyde for 10 minutes at room temperature, centrifuged, and lysed with cell lysis buffer B. A total of 1 mg of proteins from the lysate was incubated overnight in phosphate-buffered saline (PBS) 0.01% Tween-T, with 20 uL of hemagglutinin (HA) tag (C29F4) monoclonal antibody–conjugated magnetic beads (Cell Signaling, Danvers, CT). Beads were washed 4 times with PBS 0.01% Tween-T before elution in Laemmli buffer. Eluates were boiled at 100°C for 5 minutes, and Western blot was performed as previously described (22). The disabled homolog 1 (DAB1) phosphorylation assay was performed as in Lee *et al.* (39), except Reelin-enriched medium was used to stimulate primary cortical neurons instead of purified Reelin.

Fluorescence-Activated Cell Sorting, Reverse Transcriptase Quantitative Polymerase Chain Reaction, and RNA Sequencing

E17.5 cortices from embryos previously electroporated at E14.5 together with the fluorescent reporter tdTomato were dissected and processed until dissociation as previously described for neuronal cultures. Cells were resuspended in PBS, filtered through a cell strainer (70 μm, BD, Franklin Lakes, NJ), and sorted on a BD FACSAria II Cell Sorter (488–633-nm laser, 100-μm nozzle at 20 psi; BD); 1 ng of RNA per sample was used for complementary DNA preparation, according to the manufacturer instructions (PrimeScript RT, Takara Bio, Kusatsu, Japan), and a preamplification (TaqMan PreAmp Master Mix, Applied Biosystems, Foster City, CA) was performed. Real-time quantitative polymerase chain reaction (SDS 7900 HT instrument, Applied Biosystems) using the SYBR Green master mix (Applied Biosystems) was used to assess the expression level of the relevant genes. Nine RNA libraries were prepared using Nextera XT DNA (Illumina, San Diego, CA) kit corresponding to the triplicates of the three experimental conditions (*Scram* shRNA, *Dgcr2* shRNA, Rescue). Libraries were multiplexed and sequenced on an Illumina HiSEQ2000 with a setup that generates pair-end reads of 2x50 bp at an average depth of 35 million read-pairs per library.

Phosphorylation Assay: Flow Cytometry

E17.5 electroporated cortices previously electroporated at E14.5 with *Scram* shRNA + green fluorescent protein (GFP) or *Dgcr2* shRNA + tdTomato were dissected and dissociated as described previously. tdTomato and GFP samples were then mixed and split into two tubes where they were washed in 10 mL of prewarmed L-15 (2% D-Glucose, Sigma-Aldrich) and centrifuged. Cells were resuspended in 1 mL of Reelin-enriched or control Dulbecco's modified Eagle medium and incubated for 30 minutes at 37°C; 500 μL of 16% prewarmed paraformaldehyde was added to the cells for a 15-minute incubation at 37°C. Cells were centrifuged and resuspended in 70% ice-cold methanol for a 30-minute incubation on ice, before being centrifugated and resuspended in 100 μL of PBS. A total of 20 μL of RAC-alpha serine/threonine-protein kinase (AKT) and anti–extracellular signal–related kinase 1/2 (ERK1/2) antibodies were added to the cells, and the mixture was incubated for 1 hour at room temperature on a rotating wheel. Cells were washed in PBS and filtrated through a cell strainer (70 μm, BD). Cells were analyzed by flow cytometry on a CyAn ADP analyzer (Beckman Coulter, Brea, CA).

Time-Lapse Imaging

E18.5 acute brain slices were prepared as described previously (22) from embryos electroporated at E14.5. Migrating

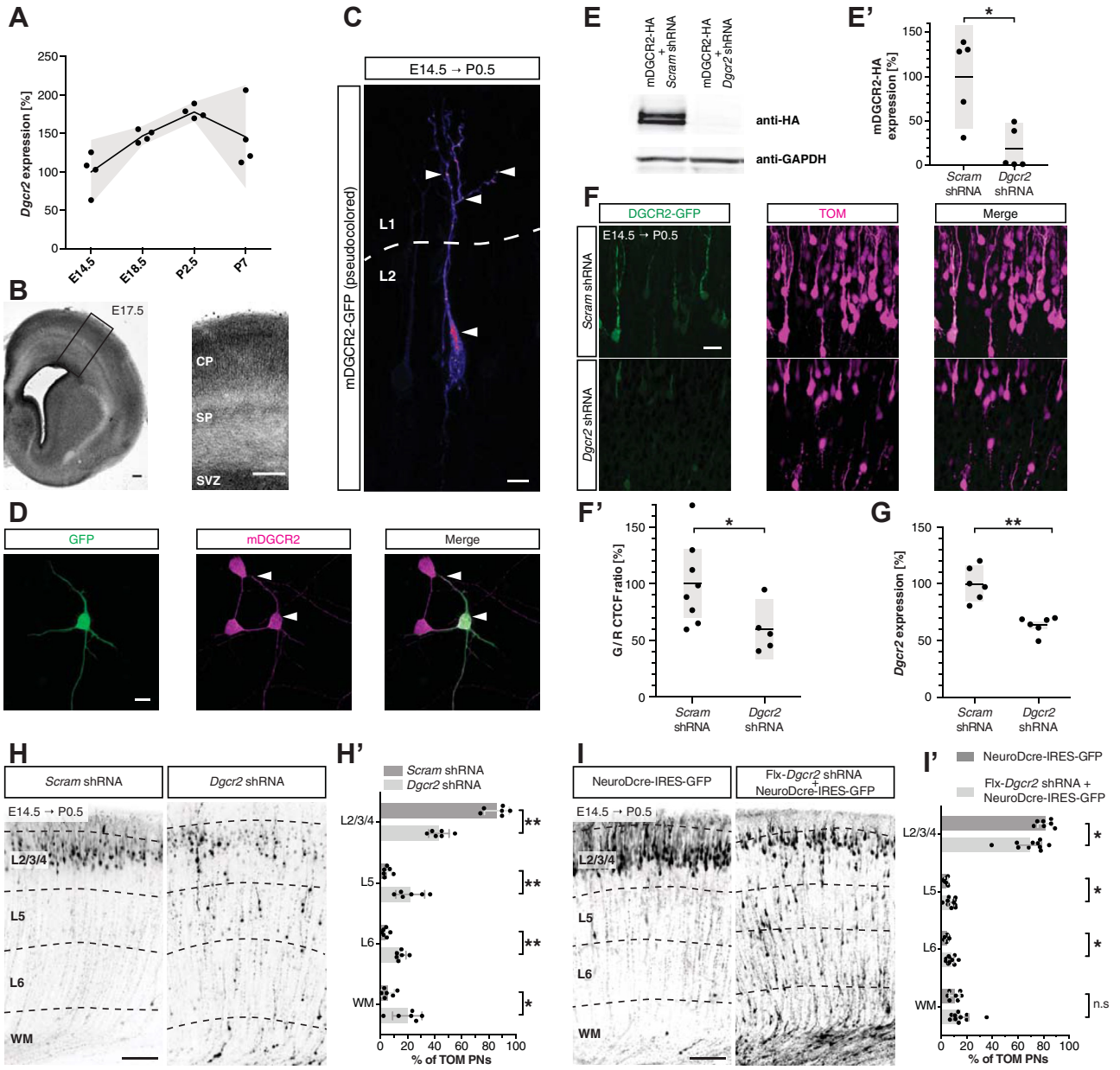

Figure 1. *Dgcr2* knockdown (KD) impairs the laminar positioning of cortical projection neurons (PNs). **(A)** Reverse transcriptase quantitative polymerase chain reaction indicates that *Dgcr2* is expressed during corticogenesis. $n = 4$ brains per time point from ≥3 separate litters. Error bar indicates 95% confidence interval (CI). **(B)** In situ hybridization reveals strong labeling of *Dgcr2* in the cortical plate (CP), subplate (SP), and subventricular zone (SVZ) of E17.5 brains. Scale bar = 100 μm. **(C)** In utero electroporation at E14.5 of a green fluorescent protein (GFP)–tagged *Dgcr2* construct in PNs. Arrowheads indicate a puncta-shaped expression of mouse DiGeorge syndrome critical region 2 (mDGCR2) (pseudocolored) localized in the cytoplasm and apical processes. Scale bar = 10 μm. **(D)** Immunohistochemistry on cultured cortical neurons demonstrates endogenous protein expression of mDGCR2 in PNs (arrowheads indicate mDGCR2 puncta). Scale bar = 10 μm. **(E/E′)** Western blot (anti-hemagglutinin [HA]) of overexpressed mDGCR2-HA in human embryonic kidney (HEK) 293T cells reveals a significant reduction of the mDGRC2-HA protein concentration, when cotransfected with a short hairpin RNA (shRNA) targeted against *Dgcr2*. $n = 5$; $p < .05$, Mann-Whitney. **(F/F′)** The corrected total cell fluorescence (CTCF) ratio between mDGCR2-GFP and tdTomato (TOM) is reduced in vivo by coelectroporation of an shRNA targeted against *Dgcr2*. $n = 5$–8 brains per condition from ≥3 separate litters. Error bars indicate 95% CI. $^*p < .05$, Mann-Whitney. Scale bar = 20 μm. **(G)** Reverse transcriptase quantitative polymerase chain reaction on RNA extracts of TOM PNs isolated by fluorescence-activated cell sorting at E17.5 after in utero electroporation at E14.5 shows that the total amount of *Dgcr2* is reduced by *Dgcr2* shRNA. $n = 6$–7 litters per condition. Error bars indicate 95% CI. $^{**}p < .01$, Mann-Whitney. **(H/H′)** shRNA-mediated *Dgcr2* KD by in utero electroporation at E14.5 dramatically impairs the laminar positioning of PNs in the somatosensory cortex at P0.5. $n = 6$ brains per condition from ≥3 separate litters. Error bars indicate 95% CI. $^*p < .05$, $^{**}p < .01$, Mann-Whitney. Scale bar = 100 μm. **(I/I′)** Conditional expression of *Dgcr2* shRNA in postmitotic PNs by coelectroporation of neurogenic differentiation–cre–internal ribosome entry site–GFP (NeuroDcre-IRES-GFP) and a lox-flanked (flx) *Dgcr2* shRNA mimics the migratory deficit observed with constitutive *Dgcr2* KD at P0.5. PNs were visualized by immunohistochemistry against GFP. $n = 7$–10 brains per condition from ≥3 separate litters. Error bars indicate 95% CI. $^*p < .05$, Mann-Whitney. GAPDH, glyceraldehyde 3-phosphate dehydrogenase. n.s., nonsignificant; WM, white matter.

PNs located in the lower part of the cortical plate (CP) at the beginning of the recording were tracked during 10 hours.

Analysis and Statistics

All described image analyses were done using Fiji (40), using the following plugins: cell counter, MtrackJ (41). The corrected total cell fluorescence was quantified on Fiji as described in Burgess *et al.* (42). Except for the RNA sequencing data, all statistical analyses were performed on GraphPad Prism software, version 7 (GraphPad Software, La Jolla, CA). The sample sizes and relevant statistical tests are specified for each result in the Results. For the detailed methods of the RNA sequencing analysis, see the Supplemental Methods.

RESULTS

Dgcr2 was found to be expressed during the late embryonic phase of corticogenesis (Figure 1A). In situ hybridization revealed that *Dgcr2* is expressed in the CP, subplate, and subventricular zone at E17.5, a period during which superficial PNs migrate toward the CP (Figure 1B). We next used in utero electroporation targeted to the E14.5 lateral ventricular zone to specifically manipulate the expression of *Dgcr2* in PN progenitors migrating toward superficial layers of the somatosensory cortex. Overexpression of a GFP-tagged *Dgcr2* construct (mouse DGCR2-GFP [mDGCR2-GFP]) in PNs showed a puncta-shaped expression in the apical processes of PNs (Figure 1C). The endogenous protein expression of *Dgcr2* was confirmed by immunohistochemistry on neuronal cultures of E14.5 electroporated PNs (Figure 1D). An shRNA targeted against *Dgcr2* significantly reduced the protein expression level of a HA-tagged *Dgcr2* (mDGCR2-HA) overexpressed in vitro in HEK 293T cells (Figure 1E). Furthermore, shRNA efficiency targeting *Dgcr2* was confirmed in vivo by measuring the fluorescence intensity of mDGCR2-GFP overexpressed in PNs (Figure 1F) and by performing reverse transcriptase quantitative polymerase chain reaction on in utero electroporated PNs isolated by fluorescence-activated cell sorting at E17.5 (Figure 1G). Overall, the shRNA-mediated KD of *Dgcr2* reduced by around 40% its messenger RNA expression.

Dgcr2 KD induced a significant alteration in the laminar positioning of PNs at P0.5, compared with a control shRNA (*Scram* shRNA). *Dgcr2*-KD PNs were significantly misplaced in the layers 5 and 6, and in the white matter (Figure 1H). This mispositioning phenotype was replicated using a second shRNA against *Dgcr2* (Supplemental Figure S1C). Furthermore, conditional expression of *Dgcr2* shRNA in postmitotic PNs induced a similar type of mispositioning phenotype (Figure 1I). *Dgcr2* KD did not alter the laminar positioning of PNs at the earlier embryonic ages of E17.5 and E18.5 (Supplemental Figure S1A, B). In addition, *Dgcr2* KD did not appear to alter the proliferation rate of PN progenitors (Supplemental Figure S2A) or their early differentiation process (Supplemental Figure S2B–E). At E15.5, the percentage of PNs that expressed the intermediate progenitor marker T-box brain protein 2 (43) in the subventricular zone was similar in the *Scram* and *Dgcr2* shRNA conditions (Supplemental Figure S2B). At E17.5, *Dgcr2*-KD PNs expressed the upper-layer markers special AT-rich sequence binding protein 2 and BRN2 (44,45), in the same proportion as control PNs (Supplemental Figure S2C, D). In addition, the percentage of electroporated PNs that expressed the deep-layer marker T-box brain protein 1 (46) remained similarly low between *Dgcr2* shRNA– and *Scram* shRNA–electroporated PNs (Supplemental Figure S2E). Overall, *Dgcr2* KD had a major impact on late PN migration but did not affect the proliferation or the early differentiation process of PN progenitors.

Dgcr2 KD induced a persistent laminar positioning deficit (Figure 2). At P7, misplaced *Dgcr2*-KD PNs were observed in deep cortical layers (Figure 2A, B) and preserved their upper-layer cut like homeobox protein cut-like 1 (CUX1) molecular identity, whereas they did not express the deep-layer marker COUP-TF-interacting protein 2 (47) (Figure 2B–D). In addition, no difference was observed in the percentage of electroporated PNs that express CUX1 in the upper layers between the *Dgcr2*-KD and control conditions (Figure 2C). Finally, at P42, misplaced *Dgcr2*-KD PNs were still observed in deep cortical layers, as opposed to control PNs (Figure 2E), and maintained expression of the upper-layer marker CUX1 (Figure 2F).

Given that the mispositioning phenotype appeared between E18.5 and P0.5, we next assessed dynamically the impact of *Dgcr2* KD on neuronal migration using confocal time-lapse imaging of PNs in E18.5 cortical slices. At this developmental time point, E14.5-born PNs are undergoing radial-guided locomotion from the upper part of the intermediate zone toward the CP (22). Quantification revealed that *Dgcr2* KD dramatically decreased the migratory speed of PNs (Figure 3A–D, Supplemental Movies S1, 2). At P0.5, *Dgcr2* KD significantly shifted the distribution of PNs to the lower CP, suggesting that *Dgcr2* KD affects the process of terminal translocation (16,20), the final step of PN migration (Figure 4A, B). To further assess the impact of *Dgcr2* KD on terminal translocation, we performed sequential in utero electroporations at E14.5 to label a reference population of control PNs and at E15.5 to assess the effects of *Dgcr2* KD on later-born PNs, which translocate in more superficial layers compared with E14.5-born PNs (20). Strikingly, E15.5-born *Dgcr2*-KD PNs were intermingled with the E14.5-born control PNs, whereas E15.5-born *Scram*-shRNA PNs were distinctly laminated in superficial layers of the CP (Figure 4C). Overall, these results indicate that radial-guided locomotion and terminal translocation of PNs are regulated by *Dgcr2*.

We next aimed to determine the molecular mechanisms through which *Dgcr2* regulates PN migration. To do this we used an in vivo electroporation rescue strategy with mouse shRNA–resistant human *DGCR2* constructs. First, we found that the *Dgcr2*-KD mispositioning phenotype was rescued by the wild-type (WT) human (h) *DGCR2* construct (Rescue WT) (Figure 5A), thus providing molecular specificity for the *Dgcr2*-KD PN migratory phenotype. Additionally, overexpression of *DGCR2* per se did not affect the laminar positioning of electroporated PNs (Supplemental Figure S1D). We then took advantage of this rescue strategy to investigate the migratory function of different subdomains of *DGCR2* (Figure 5A). Mutated constructs with deletions of the cytoplasmic C-terminal domain of *DGCR2* (C'-Del) or the extracellular low-density lipoprotein receptor class A (LDL-A) domain (LDL-Del) (Supplemental Figure S3A) did not rescue the *Dgcr2*-KD PN

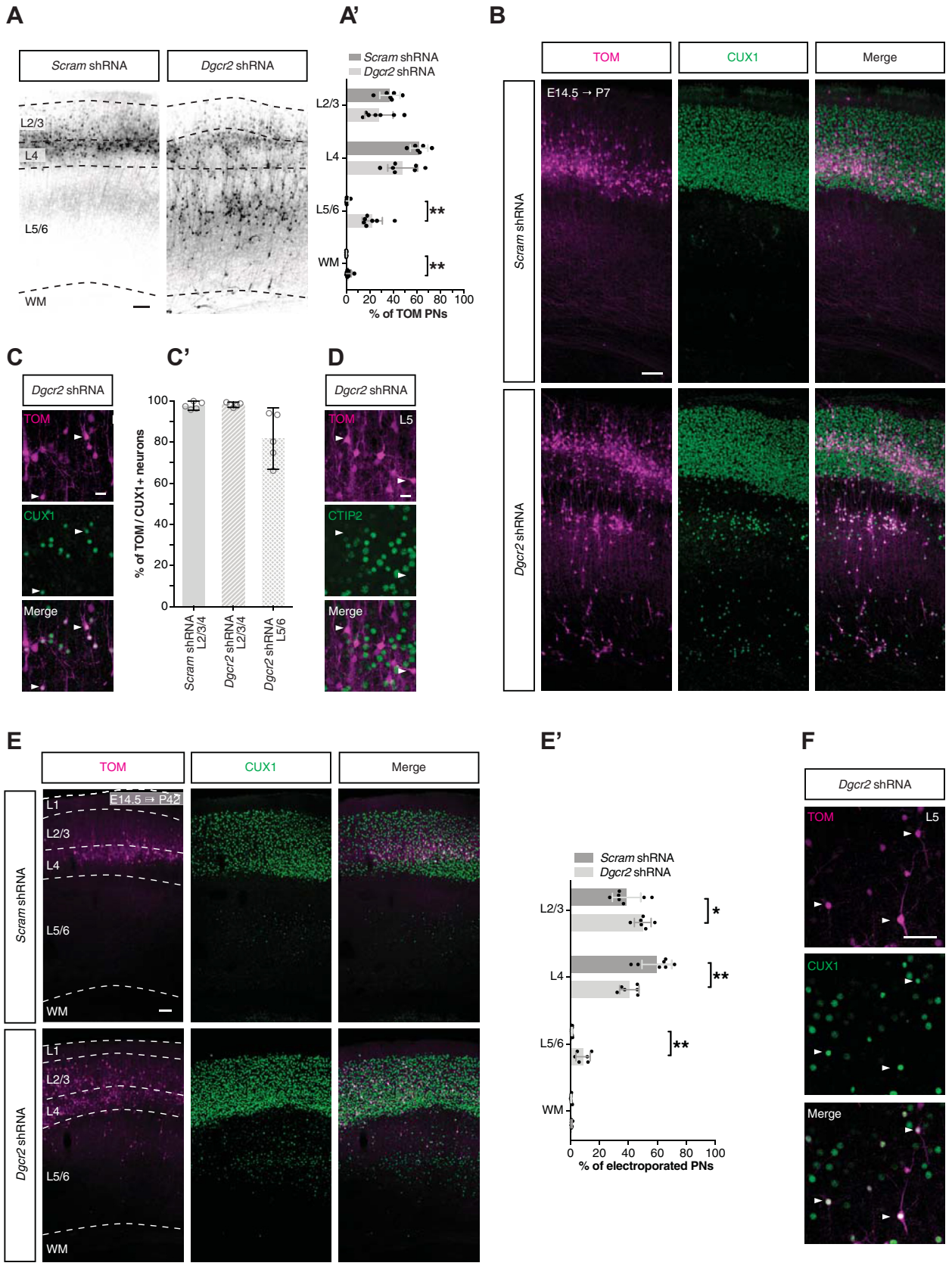
A
Scram shRNA
Dgcr2 shRNA
L2/3
L4
L5/6
WM
A'
Scram shRNA
Dgcr2 shRNA
L2/3
L4
L5/6
WM
**
**
0 20 40 60 80 100
% of TOM PNs
B
TOM
CUX1
Merge
E14.5 → P7
Scram shRNA
Dgcr2 shRNA
C
Dgcr2 shRNA
TOM
CUX1
Merge
C'
% of TOM/CUX1+ neurons
0 20 40 60 80 100
Scram shRNA L2/3/4
Dgcr2 shRNA L2/3/4
Dgcr2 shRNA L5/6
D
Dgcr2 shRNA
TOM
L5
CTIP2
Merge
E
TOM
CUX1
Merge
E14.5 → P42
Scram shRNA
Dgcr2 shRNA
L1
L2/3
L4
L5/6
WM
E'
Scram shRNA
Dgcr2 shRNA
L2/3
L4
L5/6
WM
*
**
**
0 20 40 60 80 100
% of electroporated PNs
F
Dgcr2 shRNA
TOM
L5
CUX1
Merge

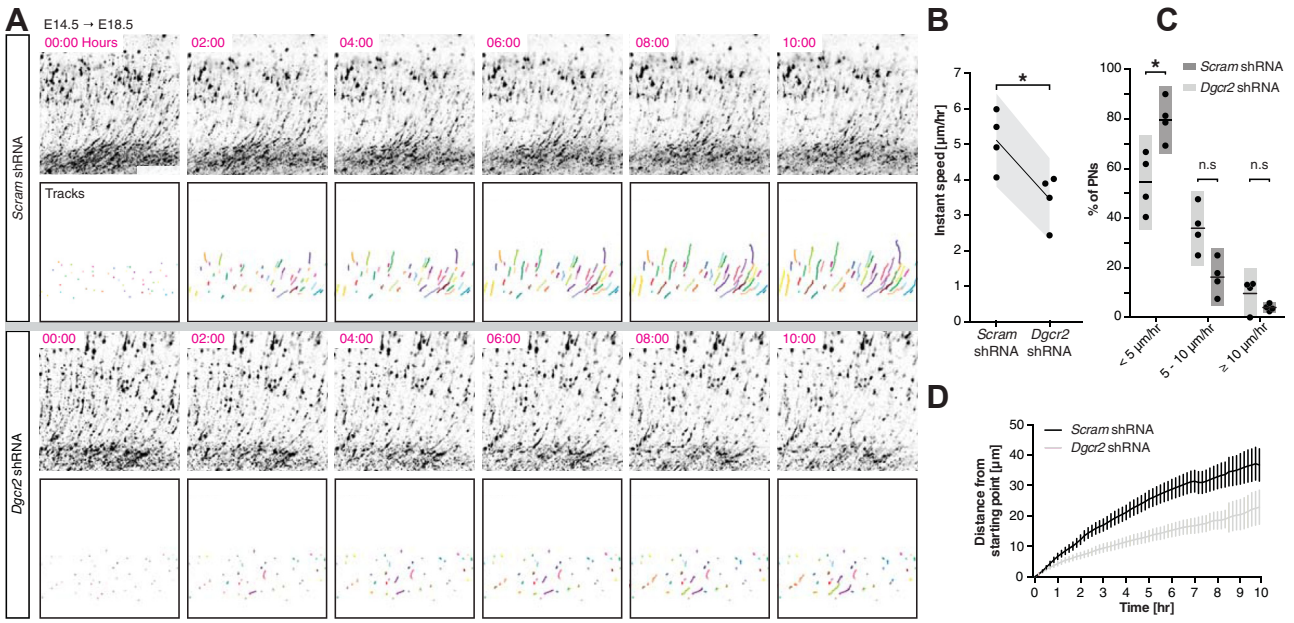

Figure 3. *Dgcr2* knockdown reduces the migratory speed of projection neurons. **(A–D)** Confocal time-lapse imaging at E18.5 of migrating projection neurons electroporated at E14.5 with tdTomato (TOM) and *Dgcr2* short hairpin RNA (shRNA) or *Scram* shRNA shows that *Dgcr2* knockdown reduces **(B)** the average instant speed, **(C)** the percentage of cells moving at high speed, and **(D)** the distance from the starting point as compared with control condition. $n = 4$ brains per condition from ≥3 separate litters, 183–196 tracked cells per condition. Color coding indicates illustrative tracked cells. Error bars indicate 95% confidence interval. $^{*}p < .05$, Mann-Whitney. Scale bar = 100 µm. n.s., nonsignificant.

migratory phenotype (Figure 5A), thus indicating that these molecular subdomains are required for human DGCR2 (hDGCR2) function in PN migration. In a more translational perspective, we also assessed the functional consequence of the SZ-risk mutation P429R (3). Strikingly hDGCR2-P429R failed to rescue the *Dgcr2*-KD migratory phenotype, providing evidence that this SZ-risk mutation is pathogenic for PN migration. Interestingly, western blots of transfected HEK 293T cells with *hDGCR2-WT-HA* or *hDGCR2-P429R-HA* revealed a significantly lower protein expression of hDGCR2-P429R-HA in contrast to WT (Figure 5B). Furthermore, overexpression of hDGCR2-P429R-HA in mouse primary cortical neurons indicated that the protein expression of hDGCR2-P429R-HA was reduced (Supplemental Figure S3B), whereas messenger RNA expression of *Dgcr2* was not modified compared with the control condition (Supplemental Figure S3C). Proteasome inhibition using MG 132, an inhibitor of the proteasome activity (48), led to a significant increase (about 60%) of hDGCR2-P429R-HA (Supplemental Figure S3D), suggesting that the SZ-risk mutation affects protein expression of *DGCR2* through increased proteasome degradation.

We next investigated the molecular mechanisms mediating the effects of DGCR2 on PN migration. Interestingly the extracellular LDL-A domain of *DGCR2* carries structural similarities with LDL-A domains found in the two canonical Reelin receptors very low-density lipoprotein receptor and apolipoprotein E receptor 2 (49). As reported (50), the canonical very low-density lipoprotein receptor coimmunoprecipitated with both full-length Reelin and the Reelin central fragment and was used here as a positive control condition (Figure 6A). Coimmunoprecipitation of Reelin with DGCR2 revealed that full length Reelin and the monomeric form of the central fragment of Reelin coimmunoprecipitated with mDGCR2 and hDGCR2, whereas no Reelin was detected in the negative control condition (GFP) (Figure 6A). Molecular proximity between DGCR2 and Reelin was further assessed in vivo using a PLA on E18.5

Figure 2. *Dgcr2* knockdown persistently affects the positioning of projection neurons (PNs) until P42 but not their laminar molecular identity. **(A/A′)** *Dgcr2* knockdown impairs the laminar positioning of E14.5-born PNs at P7. $n = 6–7$ brains per condition from ≥3 separate litters. Error bars indicate 95% confidence interval (CI). $^{**}p < .01$, Mann-Whitney. Scale bars = 100 µm. **(B)** Immunohistochemistry of the upper-layer neuronal marker cut like homeobox 1 (CUX1) at P7, after in utero electroporation of *Dgcr2* short hairpin RNA (shRNA) at E14.5, compared with *Scram* shRNA. Scale bars = 100 µm. **(C/C′)** High magnification captures of mispositioned PNs in layer 5 in the *Dgcr2* shRNA condition shows that at P7 the vast majority of misplaced PNs express the upper-layer marker CUX1. Arrowheads show colocalized PNs. $n = 5$ brains per condition from ≥3 separate litters. Error bars indicate 95% CI. Scale bars = 20 µm. **(D)** Mispositioned PNs do not express the deep-layer marker COUP-TF-interacting protein 2 (CTIP2). Arrowheads indicate electroporated PNs. Scale bars = 20 µm. **(E/E′)** *Dgcr2* knockdown impairs the laminar positioning of E14.5-born PNs at P42. $n = 6–7$ brains per condition from ≥2 separate litters. Error bars indicate 95% CI. $^{**}p < .01$, Mann-Whitney. Scale bars = 100 µm. **(F)** High-magnification image of mispositioned PNs in layer 5 in the *Dgcr2* shRNA condition shows that at P42, misplaced PNs maintain expression of the upper-layer marker CUX1. Arrowheads show colocalized PNs. Scale bars = 50 µm. TOM, tdTomato; WM, white matter.

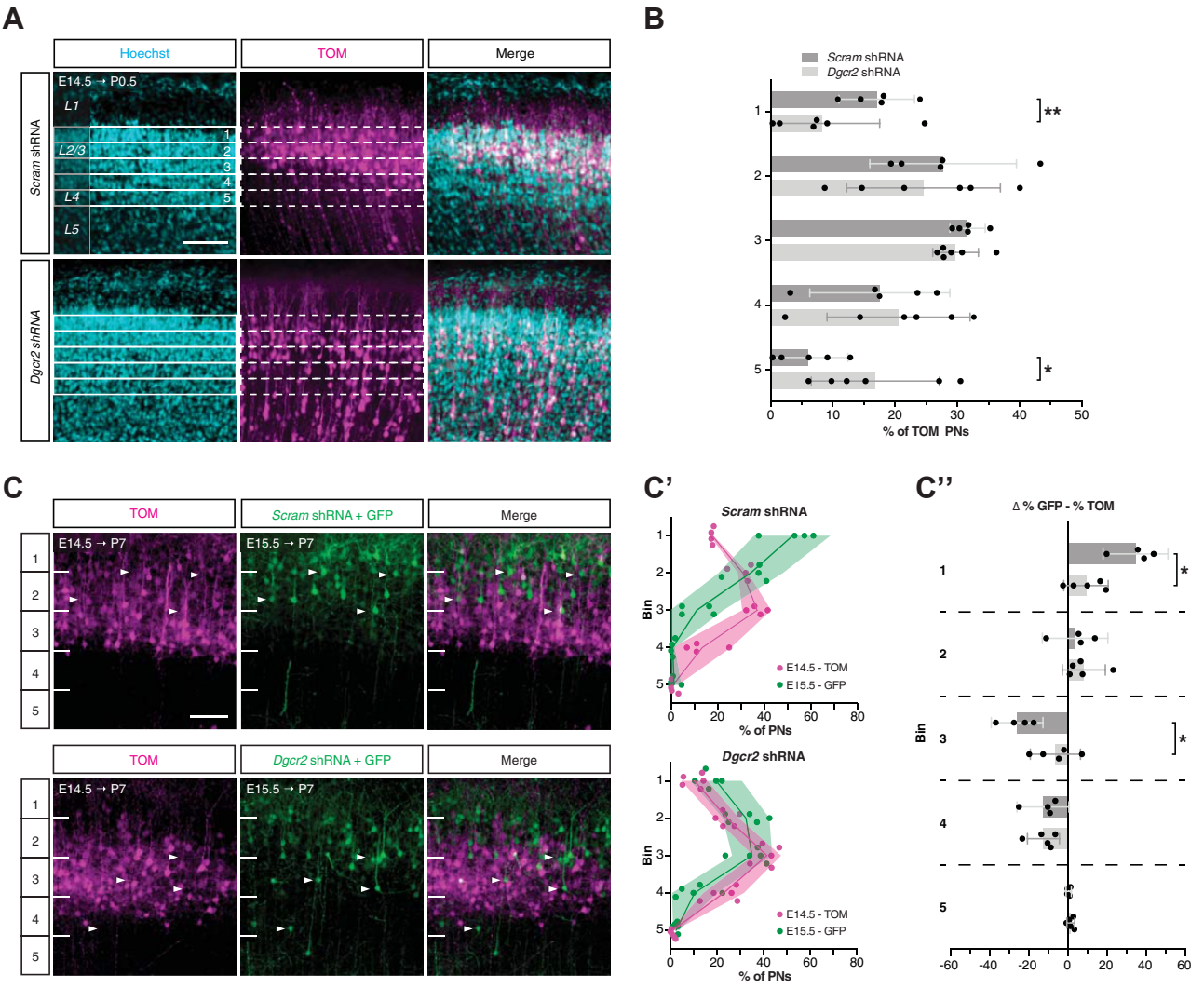

Figure 4. *Dgcr2* knockdown (KD) impairs the terminal translocation of upper-layer projection neurons (PNs). **(A, B)** *Dgcr2* KD reduces the fraction of E14.5 electroporated PNs reaching the outermost region of the cortical plate (CP) at P0.5 (Bin 1) as compared with *Scram* short hairpin RNA (shRNA). Same dataset as in Figure 1. n = 5–6 brains per condition from ≥3 separate litters. $^{*}p < .05$, $^{**}p < .01$, Mann-Whitney. Error bars indicate 95% confidence interval. **(C)** Sequential in utero electroporations of PNs at E14.5 with tdTomato (TOM) and at E15.5 with green fluorescent protein (GFP) + *Scram* or *Dgcr2* shRNA demonstrates that at P7 the inside-out laminar assembly of PNs is disrupted by *Dgcr2* KD. Arrowheads indicate E15.5 born PNs. n = 4–5 brains per condition from ≥3 separate litters. $^{*}p < .05$, Mann-Whitney. Error bars indicate 95% confidence interval. Scale bar = 100 μm.

cortical slices. We observed that the overall density of PLA puncta was highest in the marginal zone (MZ) as compared with other cortical compartments (Figure 6C), in line with observations that Reelin is mainly secreted by Cajal-Retzius cells in the MZ (51). Strikingly, we found that *Dgcr2* KD decreased PLA puncta density as compared with *Scram* shRNA condition in the MZ (Figure 6C), whereas the total protein expression of Reelin was unaffected by *Dgcr2* KD (Supplemental Figure S3E). These results provide novel evidence that DGCR2 and Reelin form a protein complex in vitro and in vivo.

To determine whether *Dgcr2* regulates Reelin signaling, we investigated the impact of *Dgcr2* KD on DAB1, a Reelin-dependent phosphorylation target controlling PN migration (52). DAB1 phosphorylation was assessed in primary neuronal cultures after stimulation with Reelin-enriched medium or mock medium using DAB1 immunoprecipitation followed by p-Y Western blot. For this experiment, *Dgcr2* KD was obtained by lentiviral infection of *Dgcr2* shRNA (Supplemental Figure S3F) in cultured neurons. In each of the five replicates of this experiment, Reelin-dependent phosphorylated DAB1 levels were decreased by *Dgcr2* KD (Figure 7A). We next performed a flow cytometry–based phosphorylation assay to assess AKT and ERK1/2, two additional Reelin-dependent phosphorylation targets (39,53). Following in utero electroporation at E14.5, control or *Dgcr2*-KD PNs were exposed at E17.5 to a Reelin-enriched medium or a control medium and the phosphorylation status of AKT (pS473) and ERK1/2 (pT202/pY204) was assessed using flow cytometry (Figure 7B).

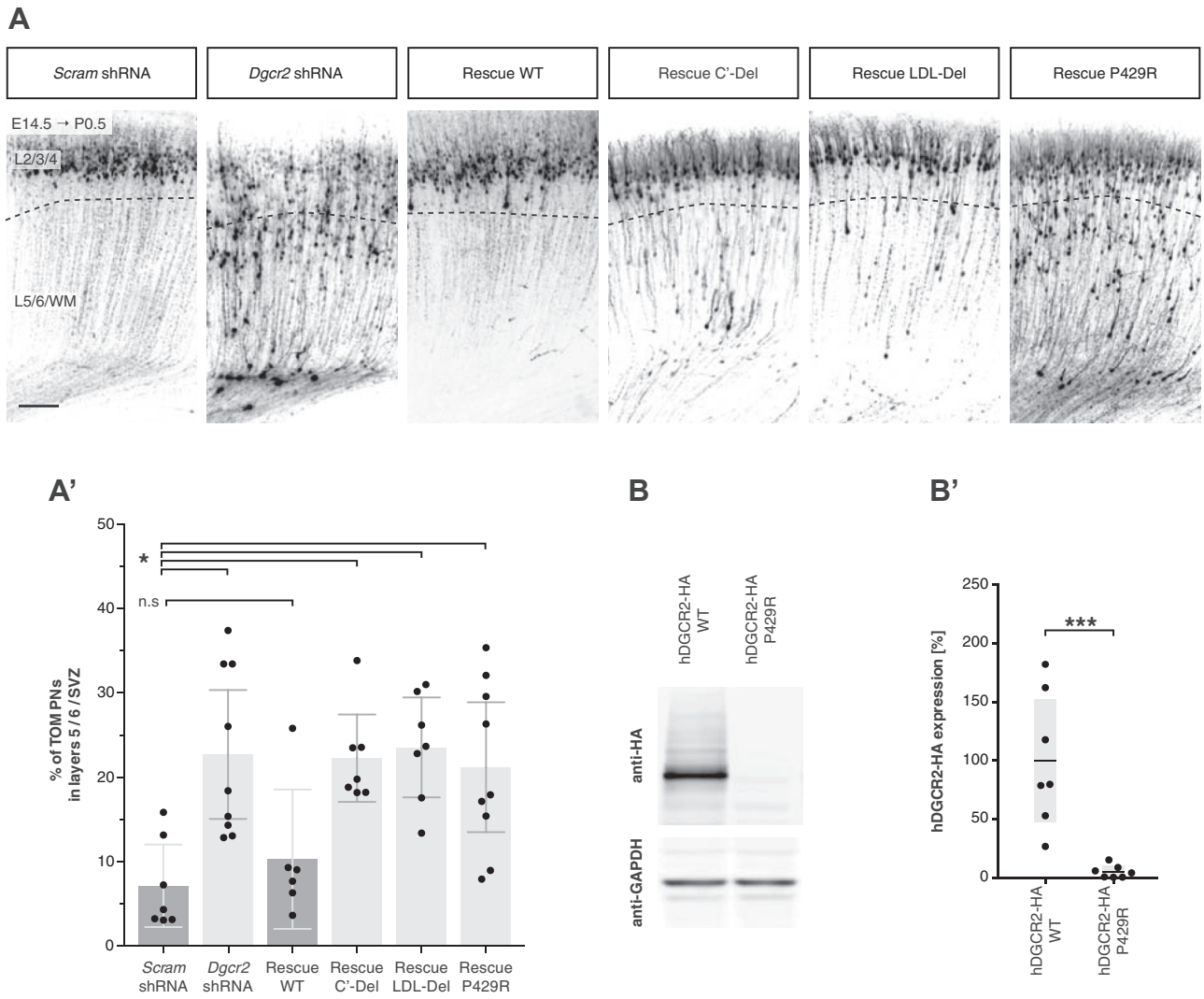

Figure 5. The human DiGeorge syndrome critical region 2 (*hDGCR2*) schizophrenia (SZ)-risk mutation does not rescue the *Dgcr2* knockdown (KD) mispositioning phenotype. **(A/A′)** Overexpression of *DGCR2* is able to rescue the positioning of projection neurons (PNs) in upper layers at P0.5, when coelectroporated with *Dgcr2* short hairpin RNA (shRNA) at E14.5 (Rescue wild-type [WT]). Deletions of the C′ terminal domain (Rescue C′-Del) or the low-density lipoprotein receptor class A (LDL-A) domain (Rescue LDL-A-Del) of *DGCR2*, as well as the missense SZ-risk mutation P429R (Rescue P429R), do not rescue the mispositioning phenotype. n = 6–9 brains per condition from ≥3 separate litters. *$p < .05$, Kruskal-Wallis + Dunn's. Error bar indicates 95% confidence interval. Scale bar = 100 μm. **(B/B′)** Western blot (anti-hemagglutinin [HA]) of protein lysates from human embryonic kidney (HEK) 293T cells overexpressing hDGCR2-WT-HA or hDGCR2-P429R-HA shows that P429R is associated with a reduced total amount of hDGCR2. n = 7. Error bars indicate 95% confidence interval. ***$p < .001$, Mann-Whitney. n.s., nonsignificant; TOM, tdTomato; WM, white matter.

Reelin-induced phosphorylation of phosphorylated AKT (Figure 7C) and phosphorylated ERK1/2 (Figure 7D) were decreased in all replicates in the *Dgcr2*-KD condition as compared with the control condition. Overall, these experiments indicate that DGCR2 is a novel member of the Reelin complex, regulating Reelin-dependent signaling targets in PNs.

To identify genetic pathways dysregulated by *Dgcr2* KD in migrating PNs, RNA sequencing was performed on PNs isolated at E17.5 using fluorescence-activated cell sorting, after E14.5 in utero electroporation. *Dgcr2* was among the top downregulated genes in the *Dgcr2*-KD condition, validating the experimental approach. Expression levels of 98 genes were found to be specifically altered in the *Dgcr2*-KD condition in contrast to the control and rescue conditions (Figure 8A, Supplemental Table S1). Interestingly, Reelin target genes (32) were significantly enriched in our dataset (p = 1.60E-04, hypergeometric testing; Figure 8A, D). Some of the *Dgcr2*-KD dysregulated genes were associated with mental disorders (54) (Figure 8B), and among them some were positively associated with psychiatric disorders such as SZ and bipolar spectrum disorders (55) (Figure 8C). Finally, Gene Set Enrichment Analysis (56) revealed that dysregulated *Dgcr2*-KD target genes were enriched in biological pathways linked to developmental

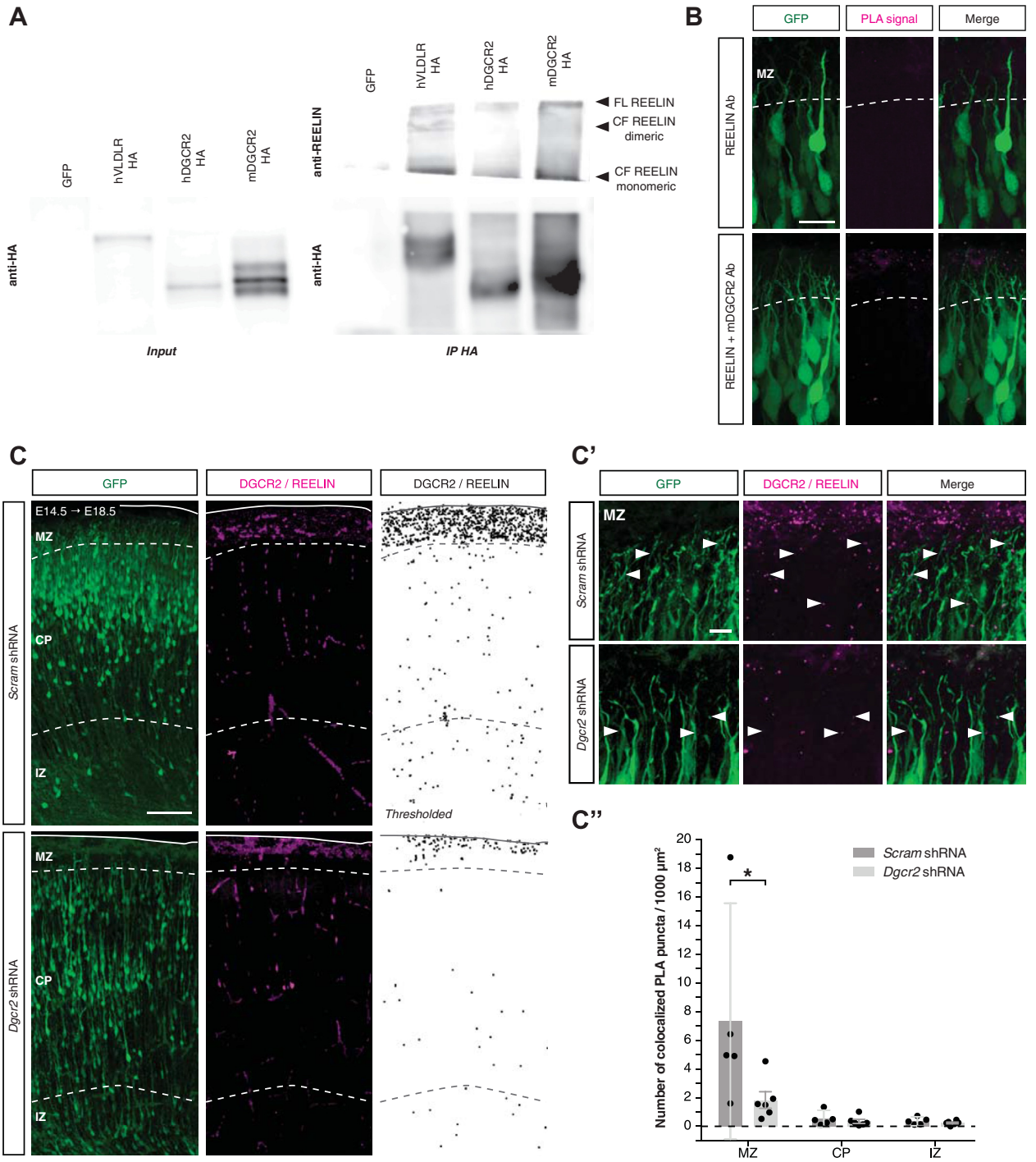

Figure 6. DiGeorge syndrome critical region 2 (DGCR2) is part of the Reelin complex. **(A)** Protein lysates from human embryonic kidney (HEK) 293T cells overexpressing green fluorescent protein (GFP), human very low-density lipoprotein receptor hemagglutinin (hVLDLR-HA), mouse DGCR2 HA (mDGCR2-HA), or human DGCR2 HA (hDGCR2-HA) were exposed to a Reelin-enriched medium and immunoprecipitated (IP) with HA. Reelin and HA were revealed by Western blot. Full-length (molecular weight > 440 kDa) Reelin and its central fragment (molecular weight = 180 kDa) coprecipitated with hVLDLR, mDGCR2, and hDGCR2 whereas the 320-kDa dimeric form of the Reelin central fragment only coprecipitated with hVLDLR. **(B)** Illustrative images of proximity ligation assay (PLA) signal on E18.5 brain slices where PLA was performed without mDGCR2 antibody (Ab) (Reelin Ab) as a negative control, compared with the test condition in which both Reelin and mDGCR2 Ab are used. Scale bar = 20 µm. **(C)** PLA on E18.5 brains electroporated at E14.5 with GFP and *Scram* or *Dgcr2* short hairpin RNA (shRNA) reveals a greater density of PLA puncta in the marginal zone (MZ) as compared with other layers of the cortex. Thresholded image

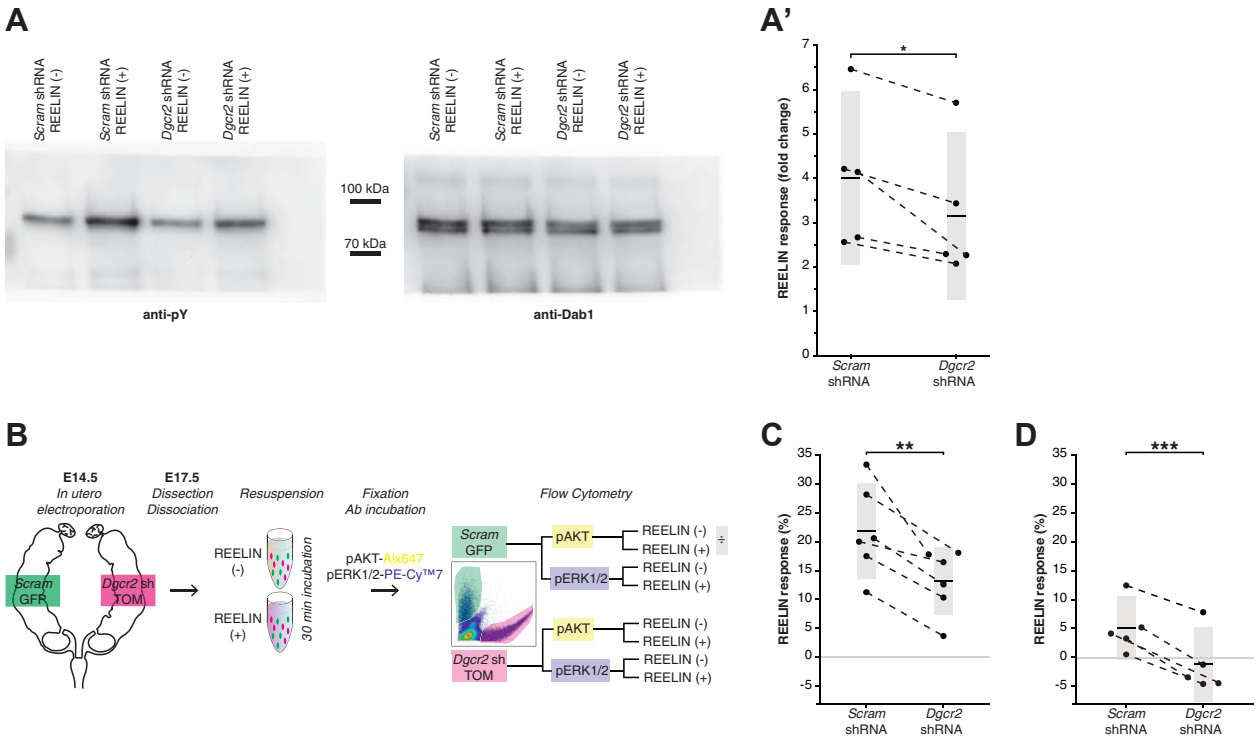

Figure 7. *Dgcr2* knockdown (KD) affects Reelin-dependent phosphorylation of disabled homolog 1 (DAB1), RAC-alpha serine/threonine-protein kinase (AKT), and extracellular signal–related kinase 1/2 (ERK1/2). **(A)** Western blot for pY and DAB1 of DAB1 immunoprecipitates shows an increased DAB1 phosphorylation in cortical neurons after exposure to a Reelin-enriched medium in the control condition, but the difference is fainter in the *Dgcr2*-KD condition. **(A′)** Quantification of the Reelin-induced phosphorylation of DAB1 in *Dgcr2*-KD cortical neurons compared with control cortical neurons, calculated as $pDAB1_{REELIN(+)}$ / $pYDAB1_{REELIN(-)}$ normalized on corresponding total DAB1, shows a decreased Reelin response in *Dgcr2*-KD cortical neurons. $^{*}p < .05$, paired *t* test. **(B)** Schematics of the flow cytometry phosphorylation assay for phosphorylated AKT (pAKT) and phosphorylated ERK1/2 (pERK1/2). Cortical projection neurons were obtained at E17.5 from somatosensory cortices of brains from the same litter, electroporated at E14.5 with green fluorescent protein (GFP) + *Scram* short hairpin RNA (shRNA) or tdTomato (TOM) + *Dgcr2* shRNA. Projection neurons were dissociated, exposed to Reelin-enriched or control medium for 30 minutes, fixed, and incubated with pAKT-Alexa 647 and pERK1/2-PE Cy7 for flow cytometry analysis. The Reelin response was assessed by the ratio of pAKT or pERK1/2 mean fluorescence between Reelin (+) and Reelin (−) conditions, expressed in percent of increase in Reelin (+). **(C)** *Dgcr2* KD reduces the Reelin-induced phosphorylation of pAKT. $n = 5$ separate litters. $^{**}p < .01$, paired *t* test. **(D)** *Dgcr2* KD reduces the Reelin-induced phosphorylation of pERK, although the average Reelin response in the control condition is only around 5%. $n = 5$ separate litters. $^{***}p < .001$, paired *t* test. pDAB1, phosphorylated disabled homolog 1.

processes and neuronal specific functions (Figure 8D, Supplemental Figure S3G, Supplemental Table S1).

DISCUSSION

Overall, this study reveals that the SZ-risk gene *Dgcr2* regulates the migration and laminar positioning of upper-layer cortical PNs. Using mutated *DGCR2* constructs, we find that the extracellular LDL-A and the cytoplasmic C′-terminal domains of DGCR2 are important molecular domains required for the migratory function of the protein. In addition, our results indicate that the missense SZ-risk mutation P429R (3) has a pathogenic effect on PN migration by leading to a state of DGCR2 protein insufficiency. Mechanistically, we show that DGCR2 is part of the Reelin complex and that *Dgcr2* KD regulates Reelin-dependent signaling pathways. Finally, using RNA sequencing we identify in migrating PNs a set of *Dgcr2*-dependent genes, which are significantly enriched in previously reported Reelin-dependent genetic targets (32).

The migration of upper-layer PNs is controlled by a variety of factors (23,24), including Reelin (57). Using time-lapse imaging and sequential electroporation in vivo we find that *Dgcr2* regulates both radial-guided locomotion as well as terminal translocation. Strikingly, the *Dgcr2-KD* PN mispositioning phenotype observed in the CP phenocopies the migratory phenotype described following in utero KD of DAB1, a key Reelin effector (20), thus suggesting that DGCR2 regulates PN migration through the Reelin signaling pathway.

represents DGCR2/Reelin PLA puncta as isolated particle $<5\ \mu m^2$ and offset by 5 pixels. PNs were visualized by immunohistochemistry against GFP. **(C′/C″)** In the MZ the number of PLA puncta that colocalize with the electroporated PNs is reduced by *Dgcr2* KD as compared with the control condition. Arrowheads depict DGCR2/Reelin PLA puncta colocalizing with GFP. $n = 5$–6 brains per condition from ≥3 separate litters. $^{*}p < .05$, Mann-Whitney. Error bars indicate 95% confidence interval. **(C)** Scale bar = 100 μm. **(C′)** Scale bar = 10 μm. CP, cortical plate; IZ, intermediate zone.

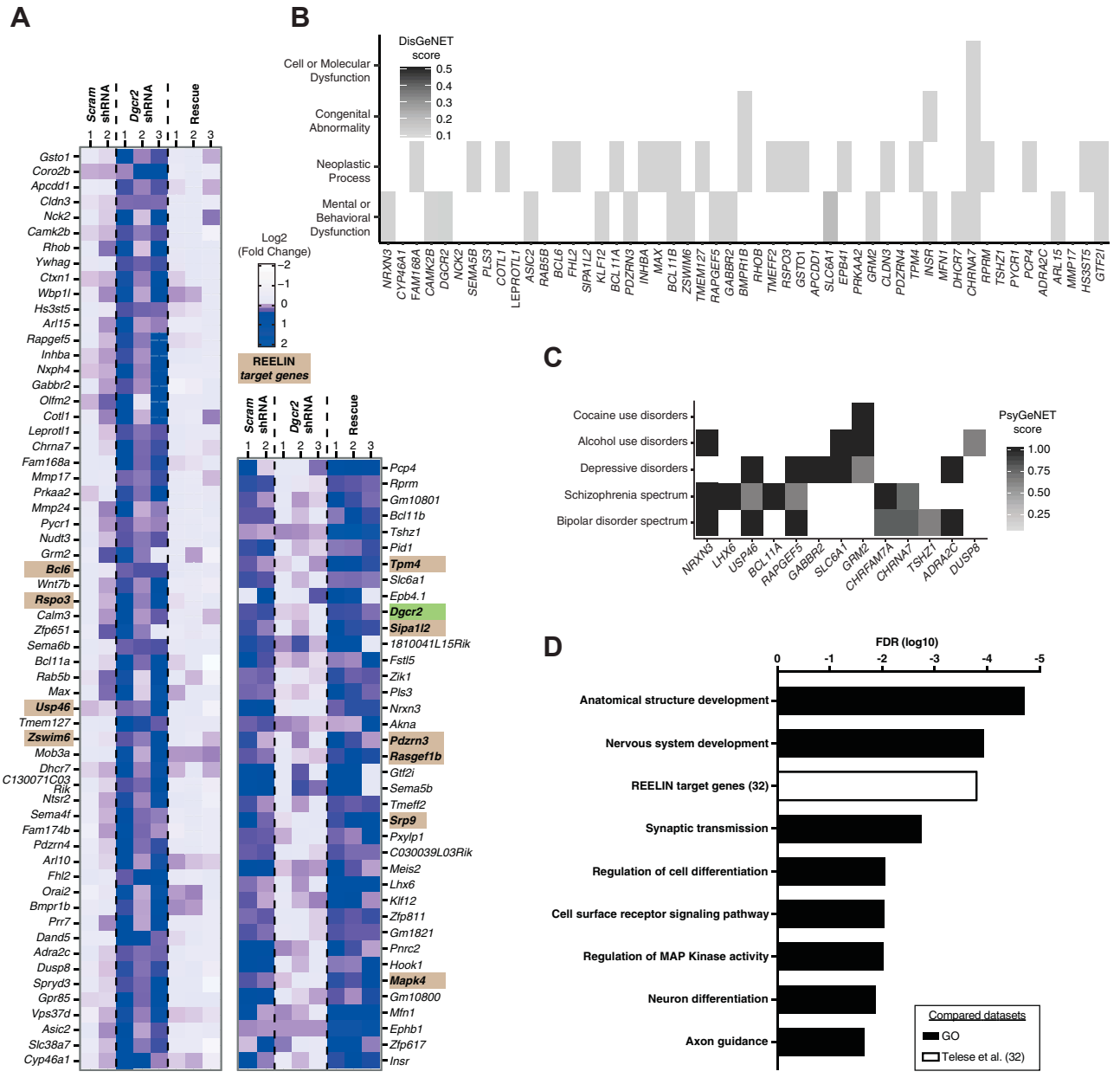

Figure 8. Transcriptional changes induced by *Dgcr2* knockdown (KD) in migrating projection neurons. **(A)** E14.5 electroporated projection neurons were isolated by fluorescence-activated cell sorting at E17.5 for RNA sequencing. Ninety-eight genes were identified as differentially expressed in the *Dgcr2*-KD condition compared with *Scram* short hairpin RNA (shRNA) or *Dgcr2* shRNA + human DiGeorge syndrome critical region 2 (hDGCR2) (Rescue). Sixty genes displayed an increased expression associated with *Dgcr2* KD and 38 displayed a decreased expression following *Dgcr2* KD. Highlighted in brown are 10 transcripts previously identified as Reelin target genes. *Dgcr2* is highlighted in green. **(B)** Selected disorders associated with *Dgcr2*-KD dysregulated genes, as identified by the DisGeNET database, encompass mental and behavioral disorders as well as congenital diseases. **(C)** PsyGeNET score highlights genes in our gene set that were positively associated with schizophrenia spectrum disorder and bipolar disorder spectrum. **(D)** Gene Set Enrichment Analysis revealed selected biological processes enriched in *Dgcr2*-KD differentially expressed genes. FDR, false discovery rate; GO, gene ontology; MAP, mitogen-activated protein.

Using coimmunoprecipitation and PLA, we reveal that DGCR2 is part of the Reelin complex. Mechanistically, we find that DGCR2 regulates Reelin-dependent phosphorylation of key intracellular effectors such as DAB1, AKT, and ERK1/2. Finally, recent work has revealed key transcriptional changes induced by Reelin activation (32). Here, we identify a core set of genes whose expression is specifically dysregulated following *Dgcr2* KD. The mitogen-activated protein kinase pathway (58,59) was enriched in the pathway analysis of *Dgcr2*-dependent genes and in this context, *Mapk4* represents an interesting

link between *Dgcr2* and Reelin (32). In addition, a significant proportion of these genes were enriched for Reelin target genes previously identified (32). Overall, these results provide evidence that DGCR2 is functionally linked to the Reelin pathway and suggests that the *Dgcr2*-KD migratory phenotype could be due to defective Reelin signaling in PNs.

Our experimental approach is based on shRNA-induced downregulation in PNs using targeted in utero electroporation. Given that this method has been reported to induce off-target effects (60), we performed rescue experiments using an *hDGCR2* construct that did not contain the mouse shRNA target sequence. The *hDGCR2* construct induced a full rescue of the shRNA-induced mispositioning phenotype, indicating the specificity of our *Dgcr2*-KD approach. In addition, this rescue approach was used to control for potential off-target gene expression changes and allowed the identification specific *Dgcr2*-KD target genes in our RNA sequencing dataset. Finally, our quantitative analysis did not detect major changes in proliferation and early neuronal differentiation following *Dgcr2* KD. However, a role for *Dgcr2* in these early developmental processes cannot be fully excluded because the efficiency of shRNA-induced KD may not be sufficiently high at these early developmental time points.

In a disease perspective, allelic variations of Reelin have been associated with SZ (61–64) and endophenotypes of SZ (65). However, single nucleotide polymorphisms and de novo mutations alone have a relatively modest effect size on the risk of developing SZ (66), compared with rare copy number variations such as 22q11.2DS (67). Among the genes encoded in this locus, *DGCR2* has been associated with SZ (3,11), although a lack of replication has been reported (68,69). More recently, an exome-sequencing study identified a potentially disruptive de novo mutation in *DGCR2* associated with idiopathic SZ (3). Here we found that this SZ-risk mutation (P429R) had a pathogenic effect on PN migration by decreasing DGCR2 protein but not transcripts levels. Decreased levels of DGCR2-P429R could be linked to increased protein degradation by the proteasome, but other mechanisms such as defective subcellular targeting or a reduced translation rate due to codon usage bias might also be involved. Overall, our results indicate that the P429R mutation could phenocopy a state of haploinsufficiency as observed in 22q11.2DS, thus suggesting that the rare de novo *DGCR2* mutation detected in a single case of idiopathic SZ (3) shares a common pathogenic mechanism with the 22q11.2DS. In a more general perspective, although numerous genetic studies provide support for an association between rare de novo mutations and SZ (3,5,70–72), this study provides, to our knowledge, the first insight into the biological pathogenicity of one of these rare mutations in vivo. SZ is conceived as neurodevelopmental disorder due to multiple pathogenic hits operating at early embryonic stages and at the later adolescent period (73). Here we display evidence that a human rare SZ-risk *DGCR2* mutation affects early steps of cortical assembly, further indicating the relevance of early embryonic hits in SZ.

The long-term effects of *Dgcr2* KD on the connectivity and circuit function of PNs will have to be assessed in future studies. Altered embryonic migration of PNs due to genetic insults has been proposed to impair their integration into cortical circuits and lead to network dysfunction as well as SZ-related behavioral deficits (74). For example, transient and selective KD of the SZ-risk gene *Disc1* in cortical PNs has been reported to affect neuronal migration (75), impair the electrophysiological properties of PNs as well as their response to dopamine pharmacological challenge, and induce SZ-relevant behavioral abnormalities, which could be reversed by clozapine (76). In addition, several studies using mouse models of 22q11.2DS have revealed developmental alterations including decreased progenitor proliferation of superficial layer PNs (77), delayed migration of hippocampal dentate progenitors (78), altered migration and distribution of parvalbumin-expressing cortical interneurons (78,79), and decreased density of superficial cortical PNs (77,80). Furthermore, at the functional level, mouse models of 22q11.2DS have revealed an imbalance between excitation and inhibition in local cortical circuits upon dopamine challenge (81), have disrupted axonal branching and synaptic transmission (82), have altered spine turnover and short-term plasticity (80), and have impaired activity patterns in neuronal ensembles (83) as well as theta- and gamma-band oscillation deficits (83,84). Whether DGCR2 plays a role in these SZ-relevant functional phenotypes remains to be determined. Finally, alterations in the distribution or density of CUX1+ superficial PNs were observed in the *Dgcr2*-KD model and in a 22q11.2DS mouse model (77,80). Given that the recent use of laminar markers revealed patches of abnormal cortical microstructure in postmortem tissue from children with autism spectrum disorders (85), similar types of investigations should be performed in human brains of 22q11.2DS patients.

In conclusion, we report that the SZ-risk gene *Dgcr2* regulates PN migration and acts through the Reelin pathway by modulating the phosphorylation of downstream effectors, and by regulating the expression of Reelin-dependent genes. Moreover, we found that a rare SZ-associated missense mutation in *DGCR2* has a pathogenic effect on PN migration, possibly by leading to a state of DGCR2 haploinsufficiency as seen in 22q11.2Del carriers. This study adds support to the hypothesis that SZ risk variants confer vulnerability to SZ by affecting early embryonic events involved in cortical circuit assembly.

ACKNOWLEDGMENTS AND DISCLOSURES

This work was supported by Swiss National Foundation Synapsy Grant No. 51NF40-158776 (to AD), Swiss National Foundation Grant No. 31003A_155896/1 (to AD), the Institute of Genetics and Genomics of Geneva (to AM-C and AD), the Fondation Privée des Hôpitaux Universitaires de Genève (to AD), and the Vachoux Foundation (to AM-C).

AM-C and AD designed the experiments and wrote the paper. AM-C performed the experiments and analyzed the data with the technical help of Dr. Julien Prados, Dr. Sabine Bavamian, Christiane Aubry-Deuel, Joan Badia Cabré, and Aurélie Flaive. The bioimaging, flow cytometry, and genomics core facilities of the University of Geneva also provided valuable technical help for this project.

The authors report no biomedical financial interests or potential conflicts of interest.

ARTICLE INFORMATION

From the Department of Psychiatry (AM-C, AD) and Department of Basic Neurosciences (AM-C, AD), University of Geneva Medical School; and the Institute of Genetics and Genomics in Geneva (AM-C, AD), University of Geneva Medical Center, Geneva, Switzerland.

Address correspondence to Alexandre G. Dayer, M.D., Departments of Psychiatry & Basic Neurosciences, University of Geneva Medical School (CMU), Rue Michel-Servet, 1, 1211 Genève 4, Switzerland; E-mail: alexandre.dayer@unige.ch.

Received Apr 6, 2017; revised and accepted Nov 6, 2017.

Supplementary material cited in this article is available online at https://doi.org/10.1016/j.biopsych.2017.11.015.

REFERENCES

1. Marín O (2012): Interneuron dysfunction in psychiatric disorders. Nat Rev Neurosci 13:107–120.
2. Shepherd GMG (2013): Corticostriatal connectivity and its role in disease. Nat Rev Neurosci 14:278–291.
3. Xu B, Roos JL, Dexheimer P, Boone B, Plummer B, Levy S, *et al.* (2011): Exome sequencing supports a de novo mutational paradigm for schizophrenia. Nat Genet 43:864–868.
4. Ripke S, Neale BM, Corvin A, Walters JTR, Farh K-H, Holmans PA, *et al.* (2014): Biological insights from 108 schizophrenia-associated genetic loci. Nature 511:421–427.
5. Xu B, Ionita-Laza I, Roos JL, Boone B, Woodrick S, Sun Y, *et al.* (2012): De novo gene mutations highlight patterns of genetic and neural complexity in schizophrenia. Nat Genet 44:1365–1369.
6. Gulsuner S, Walsh T, Watts AC, Lee MK, Thornton AM, Casadei S, *et al.* (2013): Spatial and temporal mapping of de novo mutations in schizophrenia to a fetal prefrontal cortical network. Cell 154:518–529.
7. Gratten J, Visscher PM, Mowry BJ, Wray NR (2013): Interpreting the role of de novo protein-coding mutations in neuropsychiatric disease. Nat Genet 45:234–238.
8. Maynard TM, Haskell GT, Peters AZ, Sikich L, Lieberman JA, LaMantia AS (2011): A comprehensive analysis of 22q11 gene expression in the developing and adult brain. Proc Natl Acad Sci U S A 100:14433–14438.
9. Wadey R, Daw S, Taylor C, Atif U, Kamath S, Halford S, *et al.* (1995): Isolation of a gene encoding an integral membrane protein from the vicinity of a balanced translocation breakpoint associated with DiGeorge syndrome. Hum Mol Genet 4:1027–1033.
10. Kajiwara K, Nagasawa H, Shimizu-Nishikawa K, Ookura T, Kimura M, Sugaya E (1996): Cloning of SEZ-12 encoding seizure-related and membrane-bound adhesion protein. Biochem Biophys Res Commun 222:144–148.
11. Shifman S, Levit A, Chen M-L, Chen C-H, Bronstein M, Weizman A, *et al.* (2006): A complete genetic association scan of the 22q11 deletion region and functional evidence reveal an association between DGCR2 and schizophrenia. Hum Genet 120:160–170.
12. International Schizophrenia Consortium, McQuillin A, Sklar P, Gill M, Pato CN, St Clair D, *et al.* (2008): Rare chromosomal deletions and duplications increase risk of schizophrenia. Nature 455:237–241.
13. Murphy KC, Jones LA, Owen MJ (1999): High rates of schizophrenia in adults with velo-cardio-facial syndrome. Arch Gen Psychiatry 56:940–945.
14. Tabata H, Nagata K-I (2015): Decoding the molecular mechanisms of neuronal migration using in utero electroporation. Med Mol Morphol 49:63–75.
15. Carrel D, Hernandez K, Kwon M, Mau C, Trivedi MP, Brzustowicz LM, Firestein BL (2015): Nitric oxide synthase 1 adaptor protein, a protein implicated in schizophrenia, controls radial migration of cortical neurons. Biol Psychiatry 77:969–978.
16. Nadarajah B, Parnavelas JG (2002): Modes of neuronal migration in the developing cerebral cortex. Nat Rev Neurosci 3:423–432.
17. Greig LC, Woodworth MB, Galazo MJ, Padmanabhan H, Macklis JD (2013): Molecular logic of neocortical projection neuron specification, development and diversity. Nat Rev Neurosci 14:755–769.
18. Tsai J-W, Bremner KH, Vallee RB (2007): Dual subcellular roles for LIS1 and dynein in radial neuronal migration in live brain tissue. Nat Neurosci 10:970–979.
19. Nadarajah B, Brunstrom JE, Grutzendler J, Wong RO, Pearlman AL (2001): Two modes of radial migration in early development of the cerebral cortex. Nat Neurosci 4:143–150.
20. Sekine K, Honda T, Kawauchi T, Kubo K-I, Nakajima K (2011): The outermost region of the developing cortical plate is crucial for both the switch of the radial migration mode and the Dab1-dependent "inside-out" lamination in the neocortex. J Neurosci 31:9426–9439.
21. Valiente M, Ciceri G, Rico B, Marin O (2011): Focal adhesion kinase modulates radial glia-dependent neuronal migration through connexin-26. J Neurosci 31:11678–11691.
22. Jacobshagen M, Niquille M, Chaumont-Dubel S, Marin P, Dayer A (2014): The serotonin 6 receptor controls neuronal migration during corticogenesis via a ligand-independent Cdk5-dependent mechanism. Development 141:3370–3377.
23. Kawauchi T (2015): Cellullar insights into cerebral cortical development: Focusing on the locomotion mode of neuronal migration. Front Cell Neurosci 9:394.
24. Ohtaka-Maruyama C, Okado H (2015): Molecular pathways underlying projection neuron production and migration during cerebral cortical development. Front Neurosci 9:447.
25. Ogawa M, Miyata T, Nakajima K, Yagyu K, Seike M, Ikenaka K, *et al.* (1995): The reeler gene-associated antigen on Cajal-Retzius neurons is a crucial molecule for laminar organization of cortical neurons. Neuron 14:899–912.
26. Caviness VS, Sidman RL (1973): Time of origin of corresponding cell classes in the cerebral cortex of normal and reeler mutant mice: An autoradiographic analysis. J Comp Neurol 148:141–151.
27. Yano M, Hayakawa-Yano Y, Mele A, Darnell RB (2010): Nova2 regulates neuronal migration through an RNA switch in disabled-1 signaling. Neuron 66:848–858.
28. Olson EC, Kim S, Walsh CA (2006): Impaired neuronal positioning and dendritogenesis in the neocortex after cell-autonomous Dab1 suppression. J Neurosci 26:1767–1775.
29. Franco SJ, Martinez-Garay I, Gil-Sanz C, Harkins-Perry SR, Müller U (2011): Reelin regulates cadherin function via Dab1/Rap1 to control neuronal migration and lamination in the neocortex. Neuron 69:482–497.
30. Iafrati J, Orejarena MJ, Lassalle O, Bouamrane L, Gonzalez-Campo C, Chavis P (2013): Reelin, an extracellular matrix protein linked to early onset psychiatric diseases, drives postnatal development of the prefrontal cortex via GluN2B-NMDARs and the mTOR pathway. Mol Psychiatry 19:417–426.
31. Banerjee A, Wang H-Y, Borgmann-Winter KE, MacDonald ML, Kaprielian H, Stucky A, *et al.* (2015): Src kinase as a mediator of convergent molecular abnormalities leading to NMDAR hypoactivity in schizophrenia. Mol Psychiatry 20:1091–1100.
32. Telese F, Ma Q, Perez PM, Notani D, Oh S, Li W, *et al.* (2015): LRP8-Reelin-regulated neuronal enhancer signature underlying learning and memory formation. Neuron 86:696–710.
33. Teixeira CM, Masachs N, Muhaisen A, Bosch C, Pérez-Martínez J, Howell B, Soriano E (2014): Transient downregulation of Dab1 protein levels during development leads to behavioral and structural deficits: Relevance for psychiatric disorders. Neuropsychopharmacology 39:556–568.
34. Verbrugghe P, Bouwer S, Wiltshire S, Carter K, Chandler D, Cooper M, *et al.* (2012): Impact of the Reelin signaling cascade (ligands-receptors-adaptor complex) on cognition in schizophrenia. Am J Med Genet B Neuropsychiatr Genet 159B:392–404.
35. Brosda J, Dietz F, Koch M (2011): Impairment of cognitive performance after reelin knockdown in the medial prefrontal cortex of pubertal or adult rats. Neurobiol Dis 44:239–247.
36. Riccio O, Jacobshagen M, Golding B, Vutskits L, Jabaudon D, Hornung JP, Dayer AG (2011): Excess of serotonin affects neocortical pyramidal neuron migration. Transl Psychiatry 1:e47.
37. Trifilieff P, Rives M-L, Urizar E, Piskorowski RA, Vishwasrao HD, Castrillon J, *et al.* (2011): Detection of antigen interactions ex vivo by proximity ligation assay: Endogenous dopamine D2-adenosine A2A receptor complexes in the striatum. Biotech 51:111–118.
38. D'Arcangelo G, Homayouni R, Keshvara L, Rice DS, Sheldon M, Curran T (1999): Reelin is a ligand for lipoprotein receptors. Neuron 24:471–479.

39. Lee GH, Chhangawala Z, Daake von S, Savas JN, Yates JR, Comoletti D, D'Arcangelo G (2014): Reelin induces Erk1/2 signaling in cortical neurons through a non-canonical pathway. J Biol Chem 289:20307–20317.
40. Schindelin J, Arganda-Carreras I, Frise E, Kaynig V, Longair M, Pietzsch T, *et al.* (2012): Fiji: An open-source platform for biological-image analysis. Nat Meth 9:676–682.
41. Meijering E, Dzyubachyk O, Smal I (2012): Methods for cell and particle tracking. Meth Enzymol 504:183–200.
42. Burgess A, Vigneron S, Brioudes E, Labbé J-C, Lorca T, Castro A (2010): Loss of human Greatwall results in G2 arrest and multiple mitotic defects due to deregulation of the cyclin B-Cdc2/PP2A balance. Proc Natl Acad Sci U S A 107:12564–12569.
43. Englund C, Fink A, Lau C, Pham D, Daza RAM, Bulfone A, *et al.* (2005): Pax6, Tbr2, and Tbr1 are expressed sequentially by radial glia, intermediate progenitor cells, and postmitotic neurons in developing neocortex. J Neurosci 25:247–251.
44. Britanova O, De Juan Romero C, Cheung A, Kwan KY, Schwark M, Gyorgy A, *et al.* (2008): Satb2 is a postmitotic determinant for upper-layer neuron specification in the neocortex. Neuron 57:378–392.
45. McEvilly RJ, de Diaz MO, Schonemann MD, Hooshmand F, Rosenfeld MG (2002): Transcriptional regulation of cortical neuron migration by POU domain factors. Science 295:1528–1532.
46. Bedogni F, Hodge RD, Elsen GE, Nelson BR, Daza RAM, Beyer RP, *et al.* (2010): Tbr1 regulates regional and laminar identity of postmitotic neurons in developing neocortex. Proc Natl Acad Sci U S A 107:13129–13134.
47. Molyneaux BJ, Arlotta P, Menezes JRL, Macklis JD (2007): Neuronal subtype specification in the cerebral cortex. Nat Rev Neurosci 8:427–437.
48. Gastaldello S, D'Angelo S, Franzoso S, Fanin M, Angelini C, Betto R, Sandonà D (2010): Inhibition of proteasome activity promotes the correct localization of disease-causing α-sarcoglycan mutants in HEK-293 cells constitutively expressing β-, γ-, and δ-sarcoglycan. Am J Pathol 173:170–181.
49. Yasui N, Nogi T, Takagi J (2010): Structural basis for specific recognition of reelin by its receptors. Structure 18:320–331.
50. Jossin Y, Ignatova N, Hiesberger T, Herz J, Lambert de Rouvroit C, Goffinet AM (2004): The central fragment of Reelin, generated by proteolytic processing in vivo, is critical to its function during cortical plate development. J Neurosci 24:514–521.
51. de Bergeyck V, Naerhuyzen B, Goffinet AM, Lambert de Rouvroit C (1998): A panel of monoclonal antibodies against reelin, the extracellular matrix protein defective in reeler mutant mice. J Neurosci Methods 82:17–24.
52. Lee GH, D'Arcangelo G (2016): New insights into reelin-mediated signaling pathways. Front Cell Neurosci 10. 7779–8.
53. Park TJ, Curran T (2008): Crk and Crk-like play essential overlapping roles downstream of disabled-1 in the Reelin pathway. J Neurosci 28:13551–13562.
54. Piñero J, Bravo À, Queralt-Rosinach N, Gutiérrez-Sacristán A, Deu-Pons J, Centeno E, *et al.* (2017): DisGeNET: A comprehensive platform integrating information on human disease-associated genes and variants. Nucleic Acids Res 45:D833–D839.
55. Gutiérrez-Sacristán A, Grosdidier S, Valverde O, Torrens M, Bravo À Piñero J, *et al.* (2015): PsyGeNET: A knowledge platform on psychiatric disorders and their genes. Bioinformatics 31:3075–3077.
56. Subramanian A, Tamayo P, Mootha VK, Mukherjee S, Ebert BL, Gillette MA, *et al.* (2005): Gene set enrichment analysis: A knowledge-based approach for interpreting genome-wide expression profiles. Proc Natl Acad Sci U S A 102:15545–15550.
57. Sekine K, Kubo K-I, Nakajima K (2014): How does Reelin control neuronal migration and layer formation in the developing mammalian neocortex? Neurosci Res 86:50–58.
58. O'Donnell A, Odrowaz Z, Sharrocks AD (2012): Immediate-early gene activation by the MAPK pathways: What do and don't we know? Biochm Soc Trans 40:58–66.
59. Lacar B, Linker SB, Jaeger BN, Krishnaswami S, Barron J, Kelder M, *et al.* (2016): Nuclear RNA-seq of single neurons reveals molecular signatures of activation. Nat Commun 7:11022.
60. Baek ST, Kerjan G, Bielas SL, Lee JE, Fenstermaker AG, Novarino G, Gleeson JG (2014): Off-target effect of doublecortin family shRNA on neuronal migration associated with endogenous microRNA dysregulation. Neuron 82:1255–1262.
61. Ishii K, Kubo K-I, Nakajima K (2016): Reelin and neuropsychiatric disorders. Front Cell Neurosci 10. 60–13.
62. Li W, Guo X, Xiao S (2015): Evaluating the relationship between reelin gene variants (rs7341475 and rs262355) and schizophrenia: A meta-analysis. Neurosci Lett 609:42–47.
63. Kuang WJ, Sun RF, Zhu YS, Li SB (2011): A new single-nucleotide mutation (rs362719) of the reelin (RELN) gene associated with schizophrenia in female Chinese Han. Genet Mol Res 10:1650–1658.
64. Shifman S, Johannesson M, Bronstein M, Chen SX, Collier DA, Craddock NJ, *et al.* (2008): Genome-wide association identifies a common variant in the reelin gene that increases the risk of schizophrenia only in women. PLoS Genet 4:e28.
65. Wedenoja J, Loukola A, Tuulio-Henriksson A, Paunio T, Ekelund J, Silander K, *et al.* (2007): Replication of linkage on chromosome 7q22 and association of the regional Reelin gene with working memory in schizophrenia families. Mol Psychiatry 13:673–684.
66. Sullivan PF, Daly MJ, O'Donovan M (2012): Genetic architectures of psychiatric disorders: The emerging picture and its implications. Nat Rev Genet 13:537–551.
67. Levinson DF, Duan J, Oh S, Wang K, Sanders AR, Shi J, *et al.* (2011): Copy number variants in schizophrenia: Confirmation of five previous findings and new evidence for 3q29 microdeletions and VIPR2 duplications. Am J Psychiatry 168:302–316.
68. Ishiguro H, Imai K, Koga M, Horiuchi Y, Inada T, Iwata N, *et al.* (2008): Replication study for associations between polymorphisms in the CLDN5 and DGCR2 genes in the 22q11 deletion syndrome region and schizophrenia. Psychiatr Genet 18:255–256.
69. Georgi A, Schumacher J, Leon CA, Wolf AV, Klein K, Böhenz KV, *et al.* (2009): No association between genetic variants at the DGCR2 gene and schizophrenia in a German sample. Psychiatr Genet 19:104.
70. Girard SL, Gauthier J, Noreau A, Xiong L, Zhou S, Jouan L, *et al.* (2011): Increased exonic de novo mutation rate in individuals with schizophrenia. Nat Genet 43:860–863.
71. Fromer M, Pocklington AJ, Kavanagh DH, Williams HJ, Dwyer S, Gormley P, *et al.* (2014): De novo mutations in schizophrenia implicate synaptic networks. Nature 506:179–184.
72. Xu B, Roos JL, Levy S, van Rensburg EJ, Gogos JA, Karayiorgou M (2008): Strong association of de novo copy number mutations with sporadic schizophrenia. Nat Genet 40:880–885.
73. Insel TR (2010): Rethinking schizophrenia. Nature 468:187–193.
74. Muraki K, Tanigaki K (2015): Neuronal migration abnormalities and its possible implications for schizophrenia. Front Neurosci 9:74.
75. Ishizuka K, Kamiya A, Oh EC, Kanki H, Seshadri S, Robinson JF, *et al.* (2011): DISC1-dependent switch from progenitor proliferation to migration in the developing cortex. Nature 473:92–96.
76. Niwa M, Kamiya A, Murai R, Kubo K-I, Gruber AJ, Tomita K, *et al.* (2010): Knockdown of DISC1 by in utero gene transfer disturbs postnatal dopaminergic maturation in the frontal cortex and leads to adult behavioral deficits. Neuron 65:480–489.
77. Meechan DW, Tucker ES, Maynard TM, LaMantia AS (2009): Diminished dosage of 22q11 genes disrupts neurogenesis and cortical development in a mouse model of 22q11 deletion/DiGeorge syndrome. Proc Natl Acad Sci U S A 106:16434–16445.
78. Toritsuka M, Kimoto S, Muraki K, Landek-Salgado MA, Yoshida A, Yamamoto N, *et al.* (2013): Deficits in microRNA-mediated Cxcr4/Cxcl12 signaling in neurodevelopmental deficits in a 22q11 deletion syndrome mouse model. Proc Natl Acad Sci U S A 110:17552–17557.
79. Meechan DW, Tucker ES, Maynard TM, LaMantia AS (2012): Cxcr4 regulation of interneuron migration is disrupted in

22q11.2 deletion syndrome. Proc Natl Acad Sci U S A 109: 18601–18606.

80. Fenelon K, Xu B, Lai CS, Mukai J, Markx S, Stark KL, *et al.* (2013): The pattern of cortical dysfunction in a mouse model of a schizophrenia-related microdeletion. J Neurosci 33:14825–14839.
81. Choi SJ, Mukai J, Kvajo M, Xu B, Diamantopoulou A, Pitychoutis PM, *et al.* (2017): A schizophrenia-related deletion leads to KCNQ2-dependent abnormal dopaminergic modulation of prefrontal cortical interneuron activity. Cereb Cortex 1–17.
82. Mukai J, Tamura M, Fenelon K, Rosen AM, Spellman TJ, Kang R, *et al.* (2015): Molecular substrates of altered axonal growth and brain connectivity in a mouse model of schizophrenia. Neuron 86:680–695.
83. Hamm JP, Peterka DS, Gogos JA, Yuste R (2017): Altered cortical ensembles in mouse models of schizophrenia. Neuron 94:153–167.
84. Tamura M, Mukai J, Gordon JA, Gogos JA (2016): Developmental inhibition of Gsk3 rescues behavioral and neurophysiological deficits in a mouse model of schizophrenia predisposition. Neuron 89:1100–1109.
85. Stoner R, Chow ML, Boyle MP, Sunkin SM, Mouton PR, Roy S, *et al.* (2014): Patches of disorganization in the neocortex of children with autism. N Engl J Med 370:1209–1219.